Orientation-Dispersed Apparent Axon Diameter via Multi-Stage Spherical Mean Optimization

Marco Pizzolato[1], Demian Wassermann[2], Rachid Deriche[3], Jean-Philippe Thiran[1,4], and Rutger Fick[5]

[1] Signal Processing Lab (LTS5), École Polytechnique Fédérale de Lausanne, Lausanne, Switzerland
[2] Parietal, Inria, CEA, Université Paris-Saclay, Palaiseau, France
[3] Athena, Inria, Université Côte d'Azur, Sophia Antipolis, France
[4] University Hospital Center (CHUV) and University of Lausanne (UNIL), Lausanne, Switzerland
[5] TheraPanacea, Paris, France

Abstract. The estimation of the *apparent* axon diameter (AAD) via diffusion MRI is affected by the incoherent alignment of single axons around its axon bundle direction, also known as orientational dispersion. The simultaneous estimation of AAD and dispersion is challenging and requires the optimization of many parameters at the same time. We propose to reduce the complexity of the estimation with an multi-stage approach, inspired to alternate convex search, that separates the estimation problem into simpler ones, thus avoiding the estimation of all the relevant model parameters at once. The method is composed of three optimization stages that are iterated, where we separately estimate the volume fractions, diffusivities, dispersion, and mean AAD, using a Cylinder and Zeppelin model. First, we use multi-shell data to estimate the undispersed axon micro-environment's signal fractions and diffusivities using the spherical mean technique; then, to account for dispersion, we use the obtained micro-environment parameters to estimate a Watson axon orientation distribution; finally, we use data acquired perpendicularly to the axon bundle direction to estimate the mean AAD and updated signal fractions, while fixing the previously estimated diffusivity and dispersion parameters. We use the estimated mean AAD to initiate the following iteration. We show that our approach converges to good estimates while being more efficient than optimizing all model parameters at once. We apply our method to *ex-vivo* spinal cord data, showing that including dispersion effects results in mean apparent axon diameter estimates that are closer to their measured histological values.

Keywords: diffusion MRI, axon diameter, dispersion, spherical mean

1 Introduction

Axon diameter estimation in white matter (WM) tissue is one of the most challenging tasks in Diffusion MRI (dMRI), due to demanding acquisition requirements and to the presence of confounding factors, such as axon orientational

dispersion [1]. These estimates can be improved by using complex models that account for dispersion [1]. However, the optimization of these models can be computationally expensive, since the presence of local minima often requires using global optimization strategies over a huge parameter space. Moreover, the degeneracy of the solution space further complicates the problem [2]. In this work, we propose a method inspired by alternate convex search [3] that decomposes the estimation problem into three simpler sub-problems, thus reducing the complexity while converging to desired results.

The knowledge of axon diameters in the WM tissue is important for a variety of applications, spanning from anatomical to functional imaging. In dMRI, however, based on modeling and physical considerations one could often compute estimates of an *apparent* axon diameter (AAD). The AAD can be estimated by acquiring data using strong diffusion sensitizing gradients directed perpendicularly to the axons, in combination with multiple diffusion times [4]. In some cases, a 3D acquisition is added to compensate for eventual misalignment with the principal axons bundle direction [5]. Typically, multi-compartment models composed of intra-axonal Cylinder and extra-axonal Gaussian models are used to estimate the AAD from this data [5–9]. The parameter estimation is confounded by the presence of axon dispersion around the principal diffusion direction [1]. However, the simultaneous estimation of both AAD and dispersion involves fitting many model parameters in a space that has several local minima. Classical approaches to find the global minimum in these situations use methods like brute force or differential evolution based optimization [10]. However, the computational cost of fitting models such as the one considered in this work, with many non-linear parameters, quickly becomes prohibitively expensive. The method we propose, allows for the estimation of orientation-dispersed axon diameters with reduced computational complexity.

In our proposed multi-stage spherical mean (MSSM) approach, we consider a two compartments model composed of an impermeable Cylinder [19] and a Gaussian Zeppelin, representing the intra- and extra-axonal diffusion microenvironments. This model is then dispersed over the sphere with a Watson distribution to represent orientational dispersion [12, 13]. The complete model has many free, mostly non-linear parameters: the mean apparent axon diameter, intra/extra signal fractions, parallel and perpendicular diffusivities, angular orientation, and dispersion. We propose to estimate these parameters in three main stages. In the first stage, we use multi-shell (MS) data to estimate the microenvironment model parameters with the spherical mean of each shell, in analogy with Multi-Compartment Microstructure Diffusion Imaging (MC-MDI) [14]. The signal fractions and the diffusivities estimated in this first stage are used to estimate the parameters of the Watson distribution from the MS data samples [12, 14], i.e. the orientation and the dispersion. Finally, the previous estimates are used to fix some of the corresponding parameters of the complete dispersed model which is fitted using the perpendicularly acquired data in order to estimate the mean AAD, an updated version of the perpendicular diffusivity, and the intra/extra-axonal compartment signal fractions. The newly estimated AAD and

perpendicular diffusivity are fixed as parameters of the micro-environment model of the first stage, and the process is iterated until convergence. The method is implemented using the open-source Dmipy framework for reproducible microstructure research[6] [15, 16], which facilitates the concatenation and construction of multi-compartment models in a parallelized and simple manner. We validate the approach with simulations and on a spinal cord diffusion MRI dataset with histology [17, 18]. Results show that the method accurately captures dispersion improving AAD estimates over a conventional non-dispersed estimation, showing an improved spatial correlation with histology.

2 Theory and Methods

Orientation dispersion can be taken into account by defining a microscopic axon model kernel which is then convolved with a Watson distribution to produce the orientation-dispersed axon model [13]. This is iteratively fitted to MS and perpendicular data with a three-stage procedure, where at each stage the parameter space is constrained by earlier estimates, and where at each iteration estimates are updated. We first present the model, then describe the proposed fitting procedure, and provide a description of the adopted datasets.

2.1 Orientation-dispersed axon model

The non-dispersed kernel model describes the microscopic axonal environment, and is composed of a restricted and a hindered diffusion compartments [6, 4]. The restricted compartment is described by a Gaussian Phase Approximation (GPA) cylinder [19] with diameter a, whereas the hindered compartment is described by a zeppelin [11]. Note that the choice of a zeppelin implies orientational dependence of the hindered compartment, corresponding to anisotropic diffusion profiles. The non-dispersed kernel is then convolved with a Watson distribution to give the following formulation for the signal attenuation

$$E(\cdot) = \overbrace{W(\kappa, \boldsymbol{\mu})}^{\text{Watson}} *_{\mathbb{S}^2} \overbrace{\left[\underbrace{f_h \overbrace{E_{\text{h}}(\cdot|\lambda_\perp, \lambda_\parallel)}^{\text{Zeppelin}}}_{\text{Hindered Extra-Axonal}} + \underbrace{f_r \overbrace{E_r(\cdot|\lambda_\parallel, a)}^{\text{GPA cylinder}}}_{\text{Intra-Axonal}} \right]}^{kernel} \tag{1}$$

where "$\cdot$" stands for the set of experimental variables $\mathbf{g}, \delta, \Delta$ including the gradient vector, pulse gradient duration, and separation of a PGSE sequence [20], $\boldsymbol{\mu}$ the main orientation in spherical coordinates, κ the concentration parameter of the Watson distribution $W(\cdot)$, $\lambda_\parallel \geq \lambda_\perp$ the undispersed parallel and perpendicular diffusivities of the microscopic axonal environment, and f_h, f_r the corresponding hindered and restricted signal fractions, with $f_r = 1 - f_h$. Note that both the hindered $E_h(\cdot)$ and restricted $E_r(\cdot)$ signal attenuations consider the full 3D signal, where the direction is determined by the Watson distribution.

[6] https://github.com/AthenaEPI/dmipy

2.2 Multi-Stage Spherical Mean (MSSM) optimization

We propose a multi-stage method with three optimization stages for estimating the parameters a, κ, $\boldsymbol{\mu}$, $\lambda_\parallel$, $\lambda_\perp$, and f_r of the model presented in eq. 1. At each stage, we estimate a different subset of parameters while fixing the others to initial values or to estimates obtained with a previous estimation. In this way, we obtain a cascade of simpler fittings that are computationally more efficient, and possibly less degenerate, than the global problem.

Stage 1: estimating diffusivities using shells spherical mean. The first step of the procedure uses the spherical mean of each shell of the MS dataset to estimate the parameters of the micro-environment without the influence of dispersion [14]. The kernel in eq. 1 is fitted by accounting for the spherical means of three or more shells i, $\bar{s}(b_i)$, which allows estimating the signal fraction f_r (and f_h), $\lambda_\parallel$, and $\lambda_\perp$, regardless of the FOD

$$\hat{f}_r, \hat{\lambda}_\parallel, \hat{\lambda}_\perp = \underset{f_r, \lambda_\parallel, \lambda_\perp}{\operatorname{argmin}} \|\bar{s}(b) - (1-f_r)\bar{e}_h(b, \lambda_\parallel, \lambda_\perp) - f_r \bar{e}_r(b, \lambda_\parallel, a)\|_2^2 \qquad (2)$$

where $\bar{e}_h(\cdot)$ and $\bar{e}_r(\cdot)$ are the hindered and the restricted spherical means of the corresponding hindered and restricted compartments, and where b is the b-value. Note that $\bar{e}_r$ is the dispersion-invariant signal spherical mean of a GPA cylinder, which we compute by approximation with spherical harmonic bases. The cylinder diameter a can initially be fixed to a large value, e.g. $6\mu m$, or to zero which would correspond to calculating the spherical mean signal of a stick.

Stage 2: estimating orientation and dispersion. In the second stage, we consider the full model in eq. 1, where we fix $(f_r, \lambda_\parallel, \lambda_\perp)$ to those estimated in the previous stage with eq. 2. This time, we optimize for the parameters of the Watson distribution, FOD $= W(\kappa, \boldsymbol{\mu})$ [14], minimizing the error norm of the model over the multi-shell diffusion-weighted images (DWIs)

$$\hat{\kappa}, \hat{\boldsymbol{\mu}} = \underset{\kappa, \boldsymbol{\mu}}{\operatorname{argmin}} \|S(b\mathbf{n})/S_0 - E(\kappa, \boldsymbol{\mu}|b\mathbf{n}, \hat{f}_r, \hat{\lambda}_\parallel, \hat{\lambda}_\perp)\|_2^2 \qquad (3)$$

where $S(b\mathbf{n})/S_0$ is the measured signal attenuation with S_0 being the non attenuated signal. The estimated set of parameters $\hat{\lambda}_\parallel, \hat{\lambda}_\perp, \hat{\kappa}, \hat{\boldsymbol{\mu}}$ is used to constrain the fitting of the model in eq. 1 for the next optimization stage, whereas $\hat{f}_r$ may be used as initial guess when it applies.

Stage 3: estimating the diameter using a perpendicular acquisition. The third stage optimization involves minimizing the error norm with respect to the signal attenuation measured along the perpendicular direction $\mathbf{n}_\perp$. For this reason, this is the most suitable acquisition for estimating the diameter, a, and updating the value of $\hat{\lambda}_\perp$, and of $\hat{f}_r$

$$\hat{a}, \hat{\lambda}_\perp, \hat{f}_r = \underset{a, \lambda_\perp, f_r}{\operatorname{argmin}} \|S(b\mathbf{n}_\perp)/S_0 - E(a, \lambda_\perp, f_r|b\mathbf{n}_\perp, \hat{\kappa}, \hat{\boldsymbol{\mu}}, \hat{\lambda}_\parallel)\|_2^2 \qquad (4)$$

where now all of the parameters of the model in eq. 1 have been estimated. In the following iteration, the newly estimated values $\hat{a}$ and $\hat{\lambda}_\perp$ are now fixed in eq. 2. The three stages are repeated until convergence.

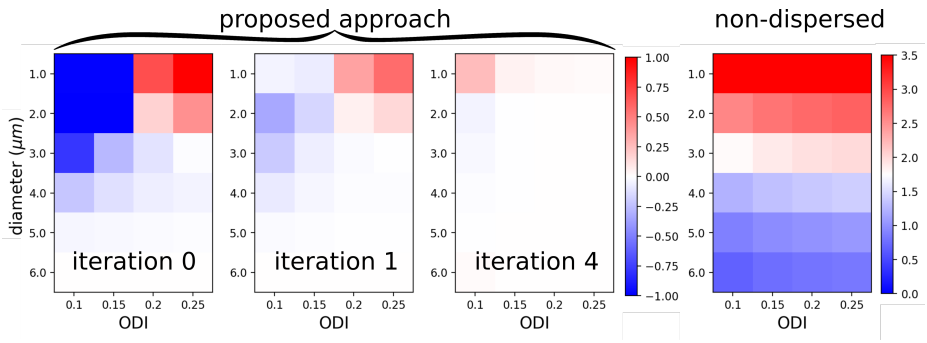

Fig. 1: Convergence of the proposed approach for a grid of parameters (diameter,ODI) over iterations (first three images). Intensities represent under (blue) and over-estimation (red). On the right, the error of the non-dispersed technique.

2.3 Implementation, MRI and Histology data

The dataset consists of a four shell DWIs collection (796 samples) and two radial acquisitions (1791 samples) with gradient direction perpendicular to the axon bundle axis of an *ex-vivo* cat spinal cord [17], which is available at the White Matter Microscopy Database [18]. Maximum gradient strength for the MS and perpendicular acquisitions were $G \approx 0.6T/m$ and $G \approx 0.85T/m$, respectively, with diffusion time $\tau = 29\,ms$ for the MS and $\tau \in \{6{,}12{,}17{,}22{,}27{,}32{,}37{,}39\}\,ms$ for the perpendicular acquisitions. Note that the data was acquired with a different echo-times for each diffusion time, which requires making some assumptions as discussed in section 4. The synthetic datasets were generated using the same acquisition scheme for consistency. Mean axon diameter histology is also present, already in MRI space. In all optimization stages we used the global MIX optimizer [10], made exception for stage 2, where differential evolution [21] was employed. All implementations were done and can be reproduced in the Dmipy software framework for reproducible microstructure research [15, 16].

3 Experiments and results

To validate our approach, we performed synthetic and acquired data experiments. In all experiments, we initialized our MSSM method with a "large" mean diameter of $6\mu m$ and let it converge in a fixed number of iterations. Results show that the proposed algorithm reaches convergence in few iterations. Moreover, obtained AAD estimates in the presence of various levels of dispersion are more precise compared to when dispersion is not modeled, as expected. The non-dispersed technique, consisting on fitting only the kernel of the model in eq. 1 with a ball instead of a zeppelin [4, 5], was informed of the angular axon bundle main direction, $\boldsymbol{\mu}$, estimated with stages 1 and 2 of the proposed method. For this reason, differences in the comparison only account for dispersion. Moreover,

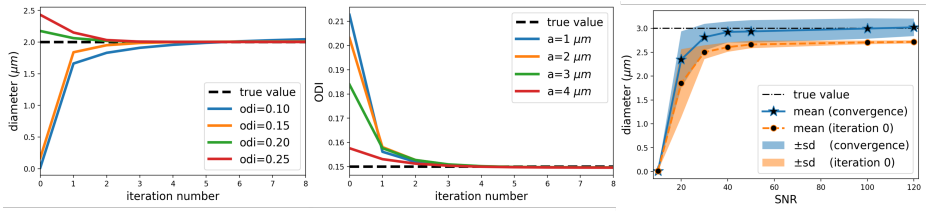

Fig. 2: Convergence of diameter and ODI estimates for proposed method over iterations. On the right, means and standard deviations of axon diameter estimates as function of the SNR, for the zeroth iteration, and at convergence.

we apply our method to the cat spinal cord dataset, where we report mean apparent axon diameter estimates closer to histological values and with comparable or better spatial correlation with respect to the non-dispersed case.

3.1 Synthetic results

We generated the synthetic signal attenuation for a grid of orientation dispersion index (ODI) values (related to κ [1]), ODI$\in \{0.10,0.15, 0.20, 0.25\}$, and cylinder diameters, $a \in \{1, 2, 3, 4, 5, 6\}\,\mu m$. For the experiment, we set $\boldsymbol{\mu} = (0, 0)$, $\lambda_{\parallel} = 1.1e-9m^2/s$, $\lambda_{\perp} = 0.8\lambda_{\parallel}$, and $f_r = 0.6$. Figure 1 reports the AAD estimation absolute error obtained with the proposed method with respect to the ground truth, for some iterations of the algorithm. We find that for smaller diameters a the error is larger. This is expected since dMRI is less sensitive to small diameters at these gradient strengths. For larger diameters and ODIs, the method converges to the correct estimates, often in just two iterations. As expected, when not accounting for dispersion, diameters are overestimated up to $3\mu m$ (fig. 1, right). We more clearly show the convergence of the method in the left and central plots of fig. 2. We also perform an evaluation of the robustness to noise for different signal-to-noise ratios, SNR$= 1/\sigma$, with σ being the standard deviation of the real and imaginary Gaussian distributions generating the added Rician noise. This evaluation is illustrated in the right plot of fig. 2, which reports the mean and standard deviation of the absolute error of the estimated diameter for the case of a $3\mu m$ apparent axon diameter with dispersion index ODI$= 0.15$. The values were obtained after repeating the MSSM method with 100 different noise realizations for each SNR, and were reported for the zeroth iteration (yellow), and at convergence (blue). The plot shows that the estimation of axon diameters converges to the right values fot SNR> 30. We believe that the suboptimal convergence at SNR=20,30 is due to the Rician bias which is not taken into account in the optimization. With respect to computational efficiency we find that one iteration of our MSSM approach takes up to $10s$, whereas a naive global implementation using MIX takes about 2 minutes for SNR=20 on a Intel® Core™ i7-3840QM with 32 Gb of RAM.

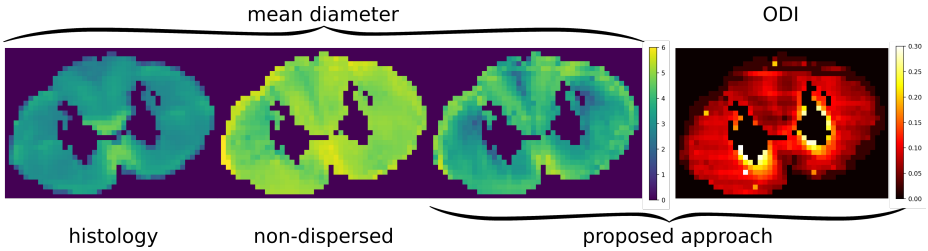

Fig. 3: Mean apparent axon diameter maps reported from histology, and calculated with the non-dispersed and with the proposed method. Right, the estimated orientation dispersion index for the proposed method.

3.2 Histological validation and comparison

Figure 3 reports the histological mean AAD maps, and the corresponding maps calculated without accounting for dispersion and for the proposed method. In the latter case, we also report the estimated dispersion index map, i.e. the ODI. The AAD map computed with the proposed method reports values clearly closer to the histology compared to the case in which dispersion is neglected. This confirms findings in the synthetic experiments. In fact, the ODI map shows a medium level of dispersion almost everywhere that the proposed method is able to capture, thus rendering apparent axon diameter estimates that are more coherent with histology. We also computed the spatial correlation between the axon diameter map obtained with the proposed method, or with the non-dispersed one, and the histology. Results that consider axons with histological diameter in range $2-5\mu m$ are shown in fig. 4. We note an improved spatial correlation and a higher dynamic range of diameter estimates obtained with the proposed method. In the same figure, we report the difference between histological and computed AAD separately for group of axons with histological diameter in range $[1-2]$, $[2-3]$, $[3-4]$, and $[4-5]$ μm, which confirms that accounting for dispersion renders estimates closer to histology.

4 Discussion, limitations, and future directions

This work presents a new method for estimating apparent axon diameters while accounting for orientational dispersion by means of a spherical mean-based multi-stage search approach. Our method reduces the complexity of the estimation compared to the naive global optimization while showing convergence. Results on *ex-vivo* data showed that the proposed approach was able to capture dispersion and render AAD estimates better aligned with histological values.

The presented method however makes some assumptions that lead to some limitations. From the point of view of modeling, we have neglected the extra-axonal diffusion time dependence [22–24]. Although assuming only intra-axonal time dependence might be a good approximation at very high gradient strengths,

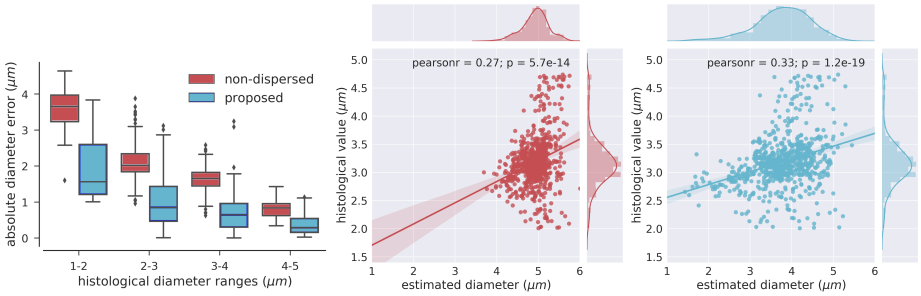

Fig. 4: The absolute AAD error estimated w.r.t. histology for the proposed (light blue) and the non-dispersed (red) methods, for increasing ranges of histological axon diameters. On the right, the correlation of MRI-based axon diameter estimates with histological values of axons with diameter in range $2-5\mu m$.

depending on the combination of (δ, Δ), at lower diffusion sensitization regimes it could possibly lead to a wrong description of the signal. In the future, we would like to account for this phenomenon by accordingly changing the extra-axonal model [22]. As a procedural limitation, we mention that the estimation of the signal fraction and diffusivities (parallel and perpendicular) obtained using shells spherical mean accounts only for the diffusion time (more generally for δ and Δ) of the MS acquisition. As a consequence, the parameters estimated at stage 1 might not be coherent with those of stage 3 where the model parameters should actually explain time dependence with respect to δ and Δ. This issue is partially mitigated for the signal fraction and the perpendicular diffusivity, since they are re-estimated at stage 3, but it is present for the parallel diffusivity and for the orientation parameters propagated through stage 2. In our synthetic results, however, we could not directly observe the effects of this phenomenon even if a more accurate investigation should be performed. This limitation could be prevented with a dataset containing MS data at different diffusion times, since the spherical mean of the cylinder, in the case of the proposed model, is dependent on diffusion time. Alternatively, in acquisitions like the one used for this work, we speculate that it could be possible to use the parameters estimated at stage 1 and 2 as initial guess for performing a gradient-descent non-linear fitting at stage 3 where all the parameters could be estimated at once. Also, the proposed processing assumes that the transverse relaxation times of the intra- and extra-axonal compartments are the same. Where this assumtion did not hold, then relaxation should be modeled. This would be particularly relevant in datasets like the one used in this work, which includes different echo-times.

In general, we point out that several choices have been made in this work that could be changed and/or improved upon. For instance, we decided to estimate $\lambda_\perp$, although initial tortuosity constraints could be imposed, as for the MC-MDI model [14], thus reducing the number of parameters. Moreover, the initialization value of the diameter could be fixed with a previous non-dispersed

fitting, and a step-size could be introduced to improve the MSSM convergence rate. At the same time, the use of global optimizers might not be necessary at each step/iteration. In addition to proposals made above, future work includes performing a more thorough comparison with global optimization results and investigating more deeply on the convergence properties of the proposed approach in order to further improve its efficiency.

5 Conclusion

In this work, we propose the use of spherical mean data to reduce the computational complexity of apparent axon diameter estimates from a compartmental model. Despite the above mentioned limitations, the adopted strategy effectively splits the estimation of a complex compartmental model into several stages leading to simpler and faster estimation steps. Further investigation is required to improve the method along this line. In fact a similar approach, eventually applied to time-dependent multi-shell data, might reveal helpful for obtaining reliable estimates in human datasets, especially where the richness of the data used for this work may not be achievable.

6 Acknowledgments

This work is supported by the Swiss National Science Foundation under grant number CRSII5_170873 (Sinergia project) and by the ERC Advanced Grant agreement No 694665 (CoBCoM).

References

1. Zhang et al.: Axon diameter mapping in the presence of orientation dispersion with diffusion MRI. NeuroImage, 56(3), 1301-1315 (2011)
2. Jelescu et al.: Degeneracy in model parameter estimation for multicompartmental diffusion in neuronal tissue. NMR Biomed, 29(1), 33-47 (2016)
3. Gorski et al.: Biconvex sets and optimization with biconvex functions: a survey and extensions. Math Method Oper Res, 66(3), 373-407 (2007)
4. Daniel Alexander: A general framework for experiment design in diffusion MRI and its application in measuring direct tissue-microstructure features. MRM (2008)
5. Alexander et al.: Orientationally invariant indices of axon diameter and density from diffusion MRI. NeuroImage, 52(4), 1374-1389 (2010)
6. Assaf et al.: AxCaliber: a method for measuring axon diameter distribution from diffusion MRI. MRM, 1347-1354 (2008)
7. Huang et al.: The impact of gradient strength on in vivo diffusion MRI estimates of axon diameter. NeuroImage, 106, 464-472 (2015)
8. De Santis et al.: Including diffusion time dependence in the extra-axonal space improves in vivo estimates of axonal diameter and density in human white matter. NeuroImage, 130, 91-103 (2016)
9. Daducci et al.: Accelerated microstructure imaging via convex optimization (AMICO) from diffusion MRI data. NeuroImage, 105, 32-44 (2015)

10. Farooq et al.: Microstructure imaging of crossing (MIX) white matter fibers from diffusion MRI. Nature Scientific reports, 6, 38927 (2016)
11. Panagiotaki et al.: Compartment models of the diffusion MR signal in brain white matter: a taxonomy and comparison. NeuroImage, 59(3), 2241-2254 (2012)
12. Kaden et al.: Parametric spherical deconvolution: inferring anatomical connectivity using diffusion MR imaging. NeuroImage, 37(2), 474-488 (2007)
13. Zhang et al.: NODDI: practical in vivo neurite orientation dispersion and density imaging of the human brain". NeuroImage, 61(4), 1000-1016 (2012)
14. Kaden et al.: Multi-compartment microscopic diffusion imaging. NeuroImage, 139, 346-359 (2016)
15. Fick et al.: Dmipy: An Open-Source Framework to improve reproducibility in Brain Microstructure Imaging. HBM (2018), https://github.com/AthenaEPI/dmipy
16. Fick et al.: Dmipy: An Open-source Framework for Reproducible dMRI-Based Microstructure Research (Version 0.1). Zenodo (2018), http://doi.org/10.5281/zenodo.1188268
17. Duval et al.: Validation of Quantitative MRI Metrics Using Full Slice Histology with Automatic Axon Segmentation. ISMRM. p. 928 (2016)
18. Cohen-Adad et al.: White Matter Microscopy Database. http://doi.org/10.17605/OSF.IO/YP4QG (2017)
19. Vangelderen et al.: Evaluation of restricted diffusion in cylinders. Phosphocreatine in rabbit leg muscle. J Magn Reson, Series B, 103(3), 255-260 (1994)
20. Tanner, J.E., and Stejskal, E.O.: Restricted Self-Diffusion of Protons in Colloidal Systems by the Pulsed-Gradient, Spin-Echo Method". JCP, 49(4), 1768-1777 (1968)
21. Storn, R., and Price, K.: Differential Evolution - a Simple and Efficient Heuristic for Global Optimization over Continuous Spaces. Journal of Global Optimization, 11, 341-359 (1997)
22. Burcaw et al.: Mesoscopic structure of neuronal tracts from time-dependent diffusion. NeuroImage, 114, 18-37 (2015)
23. Fieremans et al.: In vivo observation and biophysical interpretation of time-dependent diffusion in human white matter. NeuroImage, 129, 414-427 (2016)
24. Lee et al.: What dominates the time dependence of diffusion transverse to axons: Intra-or extra-axonal water?. NeuroImage (2017)